Environmental Effects on Parameters of Leakage Current Equivalent Circuits of Outdoor Insulators

Adjie Bagaskara [1] , Rachmawati [1, 2*] , Suwarno [1]

[1] *School of Electrical Engineering and Informatics, Institut Teknologi Bandung, Jalan Ganesa 10, Bandung, 40132, Indonesia.*

[2] *Research Center for Nanosciences and Nanotechnology, Institut Teknologi Bandung, Jalan Ganesa 10, Bandung, 40132, Indonesia.*

Abstract

The performance of outdoor insulators in transmission lines may deteriorate due to aging and can even be enhanced by the presence of pollutants. Leakage current (LC) measurement is one of the most effective methods to diagnose the insulator condition, utilizing LC parameters such as magnitude and total harmonic distortion (THD). However, research on the interpretation of these parameters is still limited. This paper discusses the diagnostic method by simulation, employing the LC equivalent circuits of different types of insulators and examining the influence of environmental factors, such as humidity and pollutant levels. LC waveforms are first obtained through experiments on various insulator types, including traditional ceramic and glass insulators, advanced composite insulators, or the hybrid type of RTV silicone rubber-coated and conducting glazed insulators. Subsequently, simulations on the LC circuits of Suwarno's and Kizilcay's models are performed to obtain similar LC waveforms and properties. The values of the equivalent circuit parameters are then used to diagnose each insulator's characteristics and environmental effects. The results indicate that composite insulators of epoxy resin or SiR have a larger intrinsic resistance of ~40 GΩ and nonlinear resistance (a few MΩ to tens of GΩ), representing high surface resistance of the insulators against water and pollutants. A comparison of these parameters is expected to indicate the severity levels of insulator condition.

1- Introduction

Insulators are critical in the electric power system, serving to isolate live parts from the grounded components. They are utilized in substations, transmission systems, and distribution systems. Various insulator types, including ceramic and polymer insulators, have distinct advantages and disadvantages in diverse environmental conditions. Particularly, outdoor insulators that are constantly exposed to environmental factors, such as pollution, humidity, rainfall, and UV light, may experience performance degradation. Over time, environmental factors can lead to flashovers or insulator failures [1]. In some regions, such as Texas in 2021 and Italy in 2013, wetting caused by ice or rain has triggered power outages [2, 3]. This is because a combination of pollutants and humidity on the insulator surface can cause dry bands to form and instigate partial discharge [4]. UV exposure can also degrade the performance of particularly polymer insulators, where constant UV radiation may decrease the hydrophobic properties as well as cause tracking or erosion on the insulator surface [5, 6]. Some environmental effects, such as the air conditioning surrounding the outdoor insulators, are commonly represented for laboratory-scale experiments by what is called salt fog and clean fog. They indicate the installation condition near coastal areas, regions with high pollution, or mountainous and highland areas.

There are various techniques for examining insulator performance and surface degradation, such as flashover voltage tests, leakage current (LC) measurements, surface tracking and erosion tests, hydrophobicity tests, and so on. Some techniques only require a visual check or can be monitored while being energized, and some others require off-line tests. Certain tests, such as thermal imaging tests using infrared cameras and partial discharge (PD) measurement tests by various sensors, can be conducted online as well. However, they only detect discharge and corona activities as indicators for the pre-flashover condition and are unable to give detailed information about insulation properties. The recent technology using thermal imaging is multimode features of active infrared thermography, conducted by Liu et al. to monitor the health of coated insulators by surface degradation or coating defects [7]. Xin et al. also identify and characterize defects in room-temperature vulcanized silicone rubber (SiR) coating on insulators quantitatively based on visible spectrum images through image processing [8].

On the other hand, the LC test is one of the most common and practical tests to determine its insulation performance since it directly reflects the intrinsic resistance or surface resistance properties of an insulator. Our previous works usually emphasize a few parameters of LC, which are LC magnitude, leakage current waveform, and harmonic components. In general, a larger cross-product between the total harmonic distortion (THD) and the magnitude of the leakage current of an insulator usually indicates a more degraded performance compared to that of new insulators with higher resistance. Waluyo et al. monitored and analyzed the daily comparative LC magnitude and determined the trend of it to evaluate the performance of porcelain and silicone rubber (SiR) insulators in natural environments, such as high humidity environments, heavy rain, or drizzle [9]. Furthermore, the distorted waveform can also be utilized to analyze the insulator's performance related to environmental factors. Salem et al. studied the LC characteristics of porcelain, glass, and silicone rubber (SiR) insulators by deriving the time domain-LC waveform in more specific waveform parameters, including the LC signal peak, the LC signal slope between two consecutive peaks, the crest factor, the phase shift between applied voltage and LC, as well as the harmonic ratio indicator to describe the severity of the pollution condition on the insulators (in terms of NSDD), which in turn can be used to predict the pre-flashover condition [10].

Nevertheless, the research on diagnostic techniques that can decipher the LC behavior into the electrical properties of insulators is very limited. Determining the electrical properties of insulators under specific conditions not only facilitates categorizing the severity of insulator conditions but also enhances our understanding of the impact of various environmental factors on the insulator's electrical properties, hence its performance. A few models in this research have been developed, where Obenaus started developing a flashover model for polluted insulators in the 1950s [11]. In 2002, Vosloo suggested an insulator model to explain the symmetrical LC waveform that occurs during dry band arcing [12]. Then Pratomosiwi & Suwarno [13] developed the electrical equivalent circuit for the insulator model which allows the creation of both symmetrical and unsymmetrical LC waveforms. Finally, this model is used in the current research to simulate the obtained LC waveforms from our past research on various types of insulators and under various environmental factors.

In our past research, the LC characteristics of uncoated ceramic insulators and RTV-SiR-coated ceramic insulators have been obtained through laboratory experiments as well as online experiments in a distribution line for 6 years in field-aged environments. LC was also measured and analyzed for semiconducting glazed (SCG) insulators, which had much larger LC flows compared to those of uncoated and SiR-coated ceramic insulators [14]. The idea of SCG application to insulators is indeed to increase the surface leakage current and, consequently, the surface temperature, aiming to repel pollutants. In addition, the most recent work is an investigation of the LC and polymeric material properties of virgin, accelerated-aged through UV radiation, as well as field-aged polymer insulators [15, 16].

This paper discusses the comparison of measured LC parameters for the previously mentioned insulator types with the addition of the LC of glass insulators and epoxy resin insulators under different environmental influences. The LC simulation results using leakage current equivalent electrical circuits are also conducted in this research using ATPDraw^{TM} software. The validation of the obtained circuit parameters is done through a comparison between the leakage current waveform properties from the simulation results and the measured ones. This work aims to obtain the intrinsic electrical properties of each insulator type and assess the impact of environmental factors, such as humidity and pollutants, on the outdoor insulators.

2- Insulator Samples, Leakage Current Measurement and Simulation Method
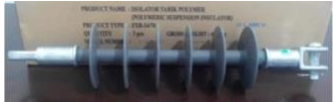
2-1- Insulator Samples

This experiment utilizes six different types of insulator samples: an RTV-SiR-coated ceramic insulator, an uncoated ceramic insulator, an epoxy resin insulator, a silicone rubber polymer insulator, a glass insulator, and a semiconducting glaze insulator. The RTV SiR coating for ceramic insulators is made by Dow Corning. The 20-kV pin-type polymer insulator is composed of epoxy resin containing 50% w/w Alumina Tri-Hydrate [ATH], while the tensile polymer insulator is constructed from silicone rubber (SiR) FXB-24/70. In the leakage current experiments, many combinations of environmental factors such as fog conditions (dry/clean fog/salt fog), pollutants, and humidity are considered. There are also virgin and aged samples, representing UV radiation exposure. However, this paper only discusses the leakage current measurement results for the insulators under clean fog conditions to focus more on pollutant effects in humid environments. Table 1 provides details on each insulator sample and the corresponding test conditions.

Table 1 illustrates variations in the conductivity of kaolin pollutants on RTV SiR-coated and uncoated ceramic insulators, quantified at 1.3 mS and 3.6 mS, following the IEC 507-1991 standard [17]. In the case of epoxy resin insulators, humidity variations include low humidity (Rh=50%-60%) and high humidity (Rh=80%-90%). Age variations are applied to SiR polymer insulators categorized as virgin and aged conditions, with the latter involving exposure to intensified UV rays, adhering to the ANSI C.29 13-2000 standard [18] for accelerated aging. The leakage current measurement for glass and semiconducting glaze insulators considers variations in kaolin pollutant levels, including no pollutant, medium pollutant (ESDD: 0.05 mg/cm^2, NSDD: 0.15 mg/cm^2), and heavy pollutant (ESDD: 0.2 mg/cm^2, NSDD: 1 mg/cm^2), as per the IEC 60507 standard [19].

Table 1. Insulator samples and test conditions

Sample No.	1	2	3
Insulator type	20 kV post-pin type Ceramic insulator with RTV silicone rubber (SiR) coating	20 kV post-pin type Uncoated Ceramic insulator	20 kV post-pin type Epoxy resin insulator
Test conditions	Pollutants' conductivity variation	Pollutants' conductivity variation	Air humidity variation

Sample No.	4	5	6
Insulator type	20 kV SiR polymer tensile insulator	Cap-pin type Glass insulator	Cap-pin type Semiconducting Glaze (SCG) insulator
Test conditions	Age variation and pollutant conductivity variation	Pollutant levels variation	Pollutant levels variation

2-2- Leakage Current Experimental Setup

Figure 1 illustrates the experimental setup for the LC measurement circuit. A 90 cm x 90 cm x 120 cm test chamber, constructed of aluminum panels, is employed to simulate environmental conditions, including pollution exposure to the samples. The insulator is placed inside the chamber, with the insulator cap connected to the HV cable. Simultaneously, the insulator pin is connected to the oscilloscope via a cable and variable shunt resistor, allowing the monitoring of LC flow on the insulator surface.
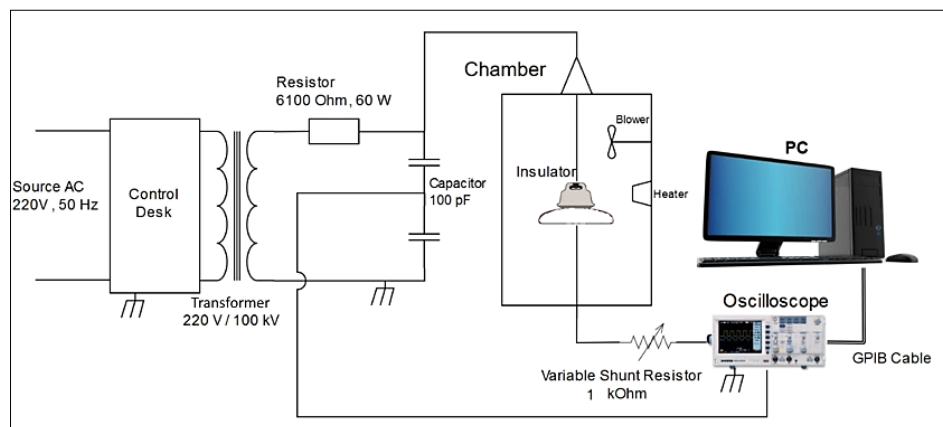

Figure 1. Insulator's leakage current measurement circuit

The LC measurement method for all insulator types follows these steps: 1) Applying AC voltage to the insulator using a step-up method ranging from 10 kV to 60 kV or less, depending on the pre-flashover condition, with a 5 kV increment at each step. 2) At each applied voltage, the LC waveform is measured and recorded in the oscilloscope. 3) Subsequently, the LC waveform data undergoes further processing using the fast Fourier transform method to obtain the LC magnitude, harmonic content, and THD for each insulator type and experimental condition. 4) After one cycle of LC measurement, the insulator is cleaned and conditioned for a different set of environmental conditions within the chamber, e.g. different humidity or different pollutants' conductivity 5) The entire process of LC measurement is reiterated until the pre-flashover condition is attained.

### 2-3- Leakage Current Modelling and Simulation Method

LC simulation employed electrical circuit simulation software integrating the Suwarno model of leakage current equivalent electrical circuit and Kizilcay's arc model [13, 20]. The Suwarno model characterizes the insulator's electrical properties, while the Kizilcay model serves as an auxiliary circuit to facilitate arc formation in the simulation. Two types of electrical equivalent circuits are used: one representing symmetrical leakage current waveforms, depicted in Figure 2-a, and the other representing unsymmetrical leakage current waveforms, as shown in Figure 2-b.

(a)   (b)
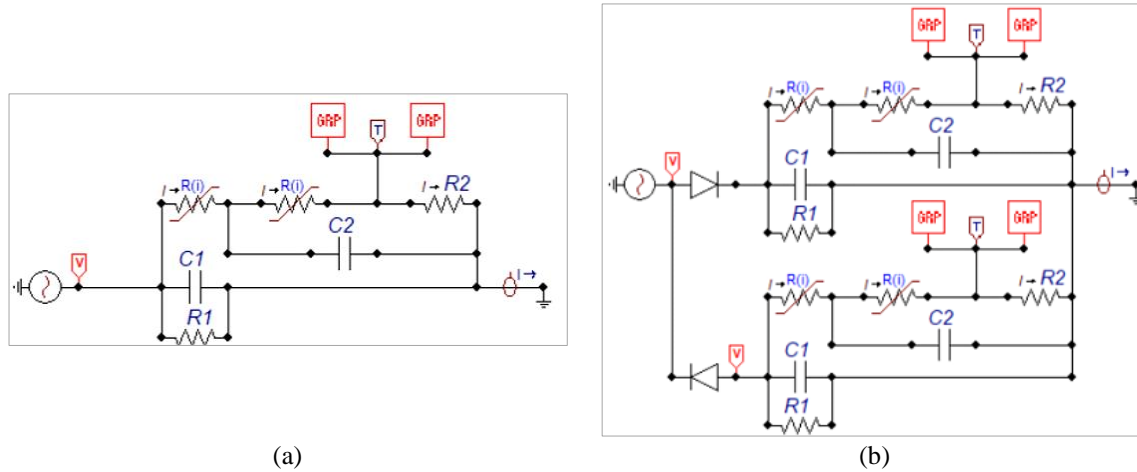
Figure 2. Insulator's electrical equivalent circuit for (a) symmetrical leakage current waveform; (b) unsymmetrical leakage current waveform

The Suwarno model equivalent circuit comprises two segments, describing the intrinsic properties and surface characteristics of the insulator. The intrinsic component features an intrinsic resistance (R1), representing the material resistivity, and an intrinsic capacitance (C1) reflecting insulator operation under high voltage. The insulator's surface is modeled by two nonlinear resistances (R(i)), a surface capacitance (C2), and a linear surface resistance (R2). In Figure 2, the left-side nonlinear resistance signifies the surface resistance in the presence of pollutants, while the right-side nonlinear resistance represents the surface resistance during dry-band discharge. Additionally, Kizilcay arc models, denoted by the "GRP" red box in Figure 2, are incorporated to induce arcs in the LC waveform of simulation results. These arc models are connected in parallel between the right-side nonlinear resistance R(i) and the linear surface resistance R2. The utilization of arc models depends on the arc types derived from the measured LC waveform and may be omitted if no arcs are evident in the waveform.

The electrical equivalent circuit is then simulated by adjusting each electrical parameter value until the simulated LC waveform aligns with that of the experimental results. Beyond waveforms, key indicators approximating insulator properties and environmental conditions include LC magnitude, THD value, and dominant harmonic numbers. The research methodology, illustrated in Figure 3, outlines the investigation of LC characteristics through a combination of experiments and simulation.
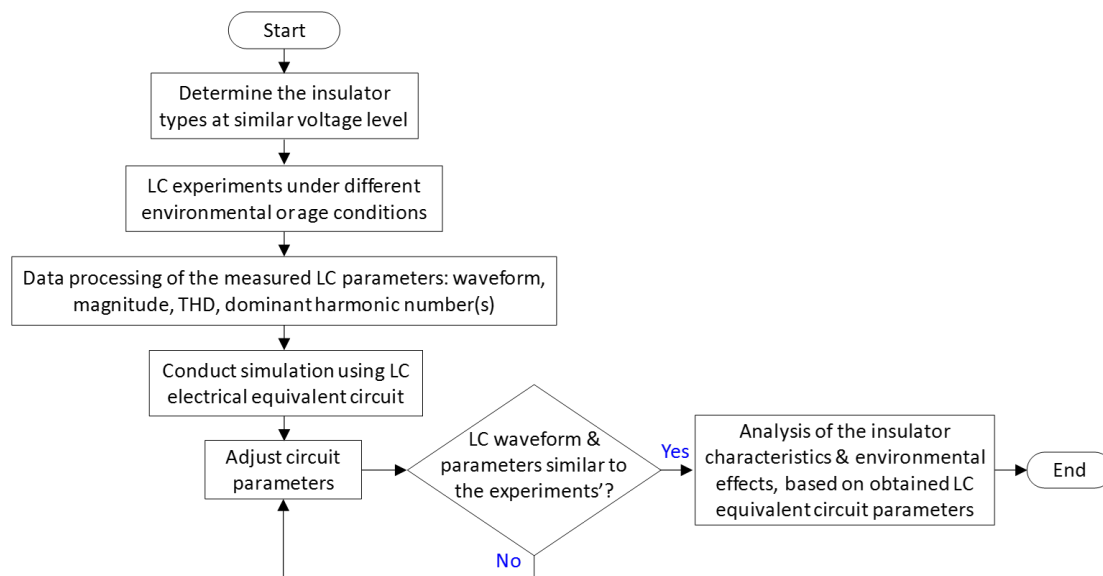

Figure 3. Flow chart of the research method

3- Leakage Current Measurement Results and Analysis

3-1- LC Measurement Results of the RTV-SiR-coated Insulator and Uncoated Ceramic Insulator

The LC experiment results on 20 kV post-pin type ceramic insulators, both with and without RTV-SiR coating are shown in Figures 4 and 5, respectively. Figures 4-a and 5-a depict the cross-products of LC magnitude (I_{LC}) and THD for the RTV-SiR coated insulator and uncoated ceramic insulators, respectively. This cross-product of I_{LC} and THD is deemed superior for insulator diagnosis due to a higher correlation factor with the severity of insulator conditions compared to I_{LC} or THD parameters alone. Additionally, Figures 4-b to 4-e and 5-b to 5-e showcase typical LC waveforms for the RTV-SiR-coated and uncoated ceramic insulators under specific environmental conditions and/or at different applied voltages.
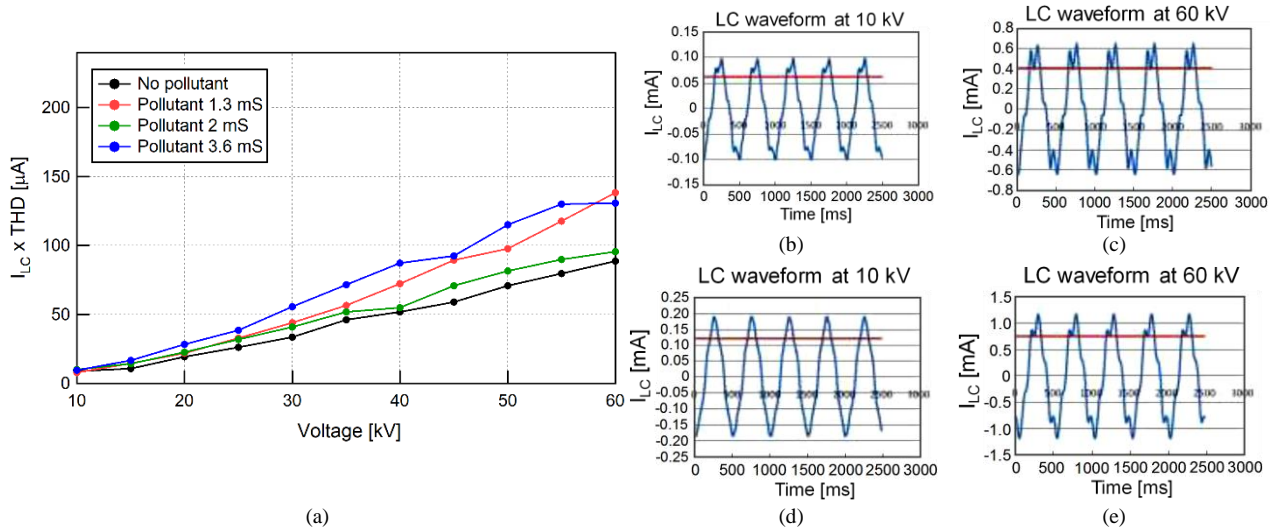
Figure 4. **(a) LC magnitude x THD of RTV SiR-coated ceramic insulator with typical LC waveform at the following conditions: (b) no to low pollutant level at lower applied voltage, (c) no to low pollutant level at higher applied voltage, (d) medium to heavy pollutant level at lower applied voltage, and (d) medium to heavy pollutant level at higher applied voltage.**
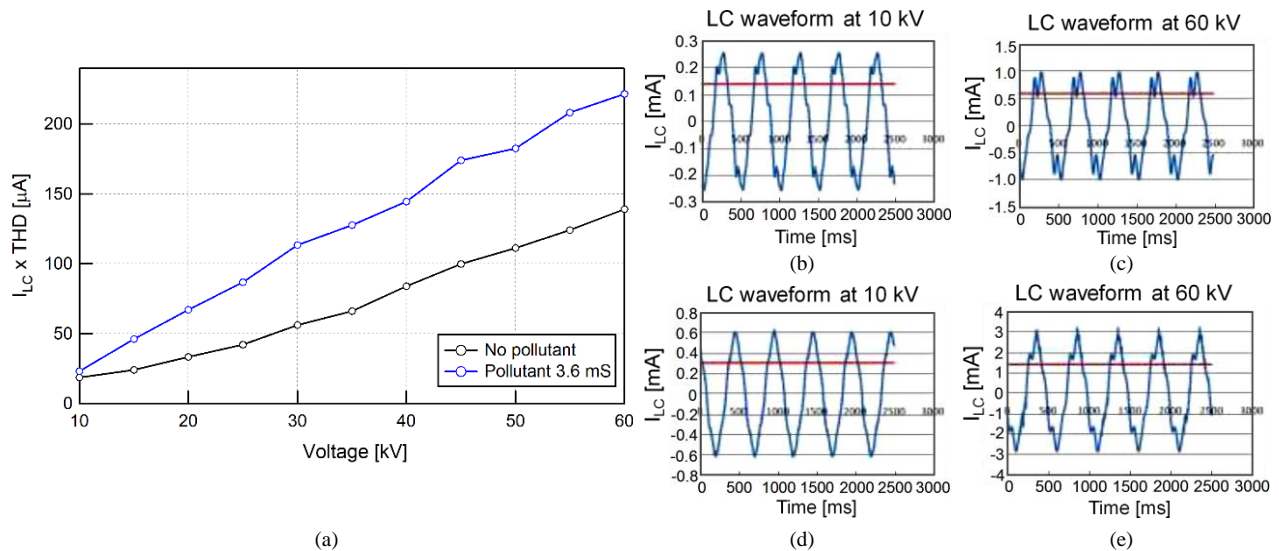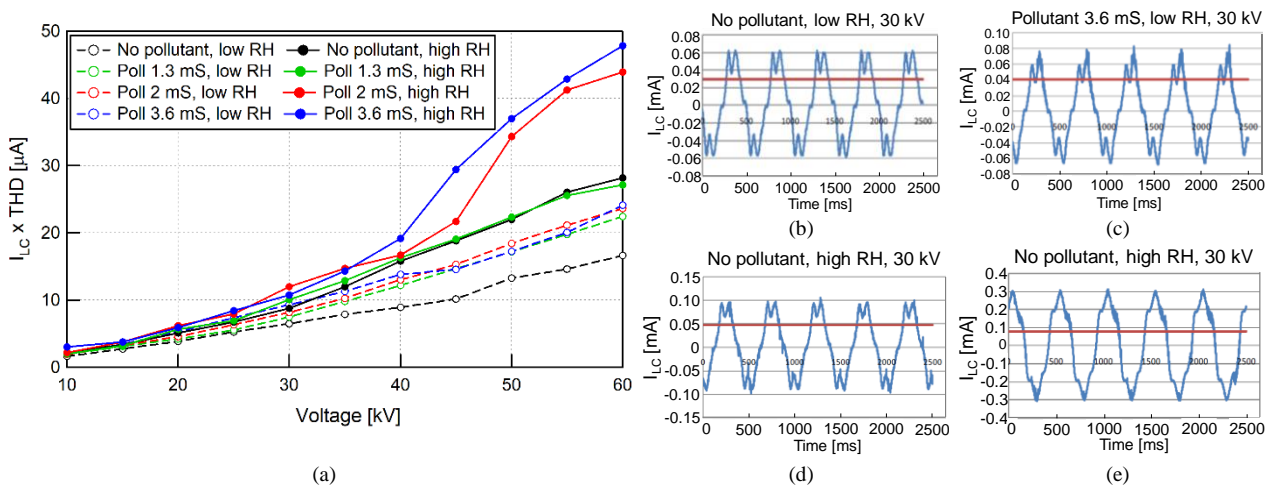

Figure 5. **(a) LC magnitude x THD of Uncoated ceramic insulator with typical LC waveform at the following conditions: (b) no pollutant level at lower applied voltage, (c) no pollutant level at higher applied voltage, (d) heavy pollutant level at lower applied voltage, and (d) heavy pollutant level at higher applied voltage.**

Examining Figures 4-a and 5-a, it is evident that the LC magnitude of both clean and kaolin-polluted samples correlates with increasing applied voltages. The quantity of kaolin pollutants, represented by the pollutants' conductivity, on the insulator surface escalates the LC magnitude for both uncoated and RTV-SiR-coated ceramic insulators. This increase is attributed to the pollutants directly enhancing the conductivity of the insulator surface by forming conduction paths. This phenomenon is well represented by the LC waveforms in Figures 4-b to 4-e and 5-b to 5-e, where the ripples at the wave crest grow larger with increasing voltage. These ripples reflect the rapid and nonlinear fluctuations resulting from dry bands due to water droplet particles on the insulator surface, causing changes in the LC wave [4, 21, 22]. From both figures, it is apparent that the application of RTV-SiR coating to ceramic insulators successfully reduced the LC magnitude, with an average decrease of 35% for no pollutant conditions and 49% for kaolin pollutants of 3.6 mS.

3-2- LC Measurement Results of the Epoxy Resin Insulator

The LC test on 20 kV pin-type epoxy resin insulators involved varying the pollutant's conductivity on the insulator surface and adjusting relative humidity (RH) levels. Figure 6(a) shows the increasing trend of the cross-product of I_{LC} and THD for the epoxy resin insulator with rising voltage under different conditions. The low and high RH in the graph imply the RH of 50%-60% and 80%-90%, respectively. The line graphs not only emphasize the impact of the pollutant quantity on the insulator surface, as discussed in the previous subsection but also highlight the influence of environmental humidity. The gradient of the LC over the voltage for insulators at low RH (0.3~0.4 mS) is smaller than that for insulators at high RH (0.5~0.9 mS) under various pollutant levels, especially at higher applied voltages. In the case of epoxy resin insulators, RH has a more pronounced effect on the LC magnitude than the amount of pollutant, particularly at higher applied voltages. This is attributed to increased condensation of water vapor on the insulator surface in a more humid environment, resulting in a larger or wider conductive layer and subsequently, an increased LC magnitude.

Furthermore, Figures 6-b and 6-b, as well as Figures 6-d and 6-e, reveal that the alteration of the LC waveform, particularly at the wave crest, is notably influenced by the conductivity of pollutants, i.e., the amount of pollutants. Over 40 kV applied voltage, the combination of high applied voltage, high pollutant conductivity, and high humidity can lead to a 2 to 3 times increase in the LC magnitude compared to conditions at low humidity.

Figure 6. (a) LC magnitude x THD of Epoxy resin insulator with typical LC waveform at the following conditions: (b) no pollutant at low RH (50-60%), (c) heavy pollutant level at low RH (50-60%), (d) no pollutant level at high RH (80-90%), and (d) heavy pollutant level at high RH (80-90%).

3-3- LC Measurement Results of the SiR Polymer Insulator

Subsequently, LC tests were conducted on two types of SiR polymer tensile insulators, namely the virgin sample and the aged sample, aiming to explore the aging and pollutant effects on aged insulators. Additionally, the exposure of insulators to UV radiation during the aging process allows for the examination of the UV radiation effect. The results of LC measurements on virgin and aged SiR insulators are presented in Figure 7. Figure 7-a displays the cross-product of I_{LC} and THD for the SiR polymer insulator, while Figures 7-b to 7-e show the typical LC waveforms under different conditions.
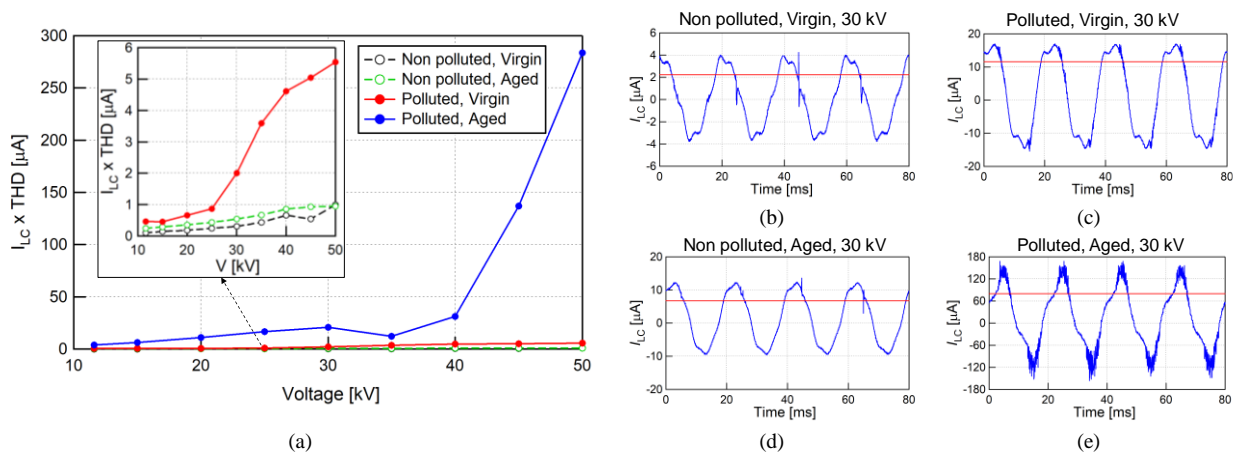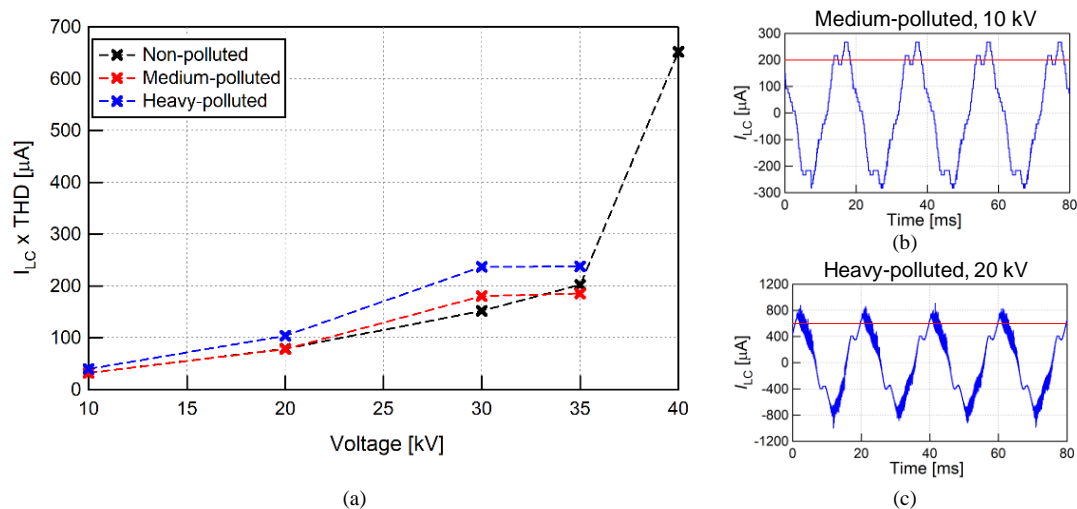

Figure 7. (a) LC magnitude x THD of SiR polymer insulator with typical LC waveform at the following conditions: (b) non-polluted and virgin, (c) polluted and virgin, (d) non-polluted and aged, and (d) polluted and aged

Figure 7-a indicates that, for non-polluted insulators, the LC gradient over increased voltage remains small for both the virgin and aged samples. However, the presence of pollutants on the insulator surface increases the LC magnitude gradient at applied voltages above 25 kV. At this stage, even the virgin and polluted insulator still performs under normal conditions. Nevertheless, the presence of a high quantity of pollutants on the aged insulator surface has a more significant impact on degrading insulation performance. This is evidenced by the amplified LC magnitude and THD due to increased arcing activity on the aged insulator sample, as shown in Figure 7-e. For instance, at 30 kV, the LC magnitude of the aged sample increases from 6.7 µA with no pollutants to 80 µA with pollutants, and the THD is enhanced from 8.1% with no pollutants to 25.8% with pollutants. The degradation in this case results from the aged and polluted insulator surface condition, which is rough and highly contaminated, impeding its ability to repel water or contaminants effectively [15].

3-4- LC Measurement Results of the Glass Insulator

Figure 8 below shows the LC measurement results for the glass insulator, encompassing the cross-product trend of the I_{LC} and THD in Figure 8-a, along with typical LC waveforms for medium-polluted and heavy-polluted insulator surface conditions in Figures 8-b and 8-c, respectively. Notably, for the non-polluted sample, the insulator continued to function normally even with a significantly large LC magnitude at 40 kV. However, both the medium-polluted and heavy-polluted insulator samples operated normally only up to 35 kV, and experiencing flashover at 40 kV. At 10 kV applied voltage, both the medium-polluted and heavy-polluted insulator samples exhibited an LC waveform with a shape similar to that in Figure 8-b, featuring two crests and symmetrical positive and negative cycles. However, as the applied voltage increased from 20 to 35 kV, more arcs occurred, starting from the second crest to the equilibrium, as depicted in Figure 8-c. The THD at this range of applied voltage ranges from 17 to 34%, showing a high distortion level of the LC waveform. This phenomenon results from increased discharge activities or arcs forming on dry bands with a rising applied voltage. Consequently, at 35 kV, for instance, the arc magnitude becomes substantial enough to distort the waveform and hence reduce the LC magnitude.

Figure 8. (a) LC magnitude x THD of Glass insulator with typical LC waveform at the following conditions: (b) medium-polluted, and (c) heavy-polluted

3-5- LC Measurement results of the Semiconducting Glazed insulator

Figure 9-a illustrates the cross-product of I_{LC} and THD for the semiconducting glazed (SCG) insulator sample under non-polluted, medium-polluted, and heavy-polluted conditions. As depicted in Figures 9-b and 9-c, the range of LC magnitude for the SCG insulator is in the order of a few mA (thousands of µA), i.e., 700–3000 µA. It is due to the semiconducting compound of tin oxide (SnO_2) presence in the SCG coating layer, which, by its material properties, amplifies the LC magnitude on the SCG insulator surface [23, 24]. The development of SCG insulators aims to increase the LC magnitude on the insulator surface, thereby raising the surface temperature. This increase in temperature or warmer surface is expected to facilitate the evaporation and repulsion of water particles containing pollutants on the insulator surface.
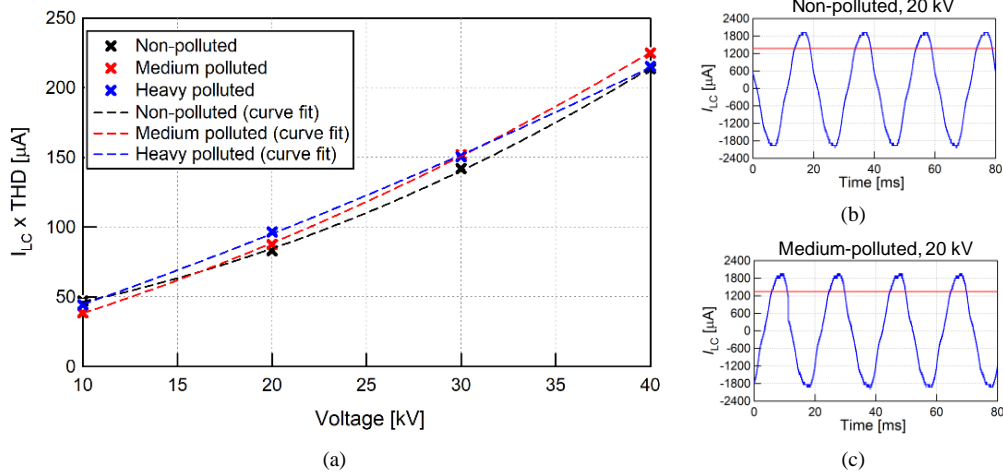
Figure 9. (a) LC magnitude x THD of Semiconducting glazed insulator with typical LC waveform at the following conditions: (b) non-polluted, and (c) medium-polluted

Figure 9-a further indicates that the LC magnitude, along with the cross product of I_{LC} x THD, only varies slightly for non-polluted, medium-polluted, and heavy-polluted SCG insulators at each applied voltage. The LC waveform is also typical for SCG insulators, with no ripples detected on the wave crest at all applied voltages, as shown in Figures 9-b and 9-c. The THD value of SCG insulator LC waveforms is much lower than that of other insulator types, ranging only around 5-7%, regardless of the pollutant levels. These observations suggest that the pollutant effect on SCG insulators is relatively small.

4- Leakage Current Simulation Results

4-1- LC Simulation Results of the RTV-SiR coated Insulator

Table 2 presents the measured LC profiles from experiments, along with the corresponding simulated profiles for the RTV-SiR-coated ceramic insulator with pollutants' conductivity of 1.3 mS and 3.6 mS. The table also includes the equivalent electrical circuit parameters representing the respective insulator conditions.

Table 2. Comparison of LC profiles between experimental and simulated results for RTV-SiR coated ceramic insulator with varying pollutants' conductivity

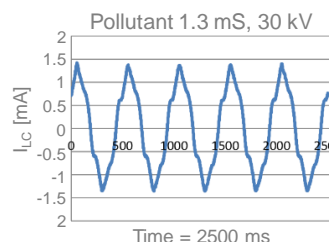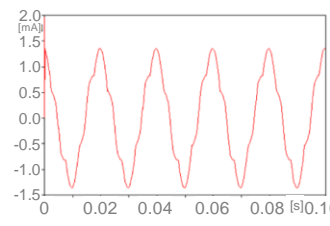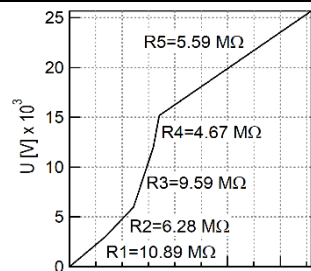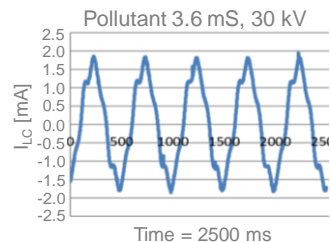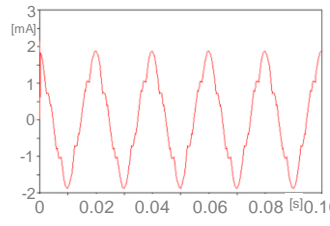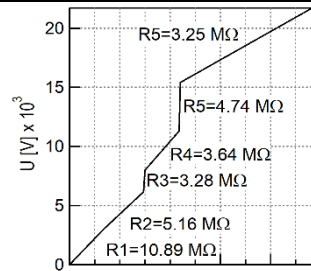| Leakage Current (LC) of Experiment	LC of Simulation	Electrical circuit parameters		
			R1(GΩ)	4.421
			R2(GΩ)	0.3
			C1(pF)	20
			C2(pF)	0.1
I_{max} = 0.35 mA, THD = 19.71%, 5th dominant	I_{max} = 0.35mA, THD = 19.72%, 5th dominant	$R_{nonlinear}$ range = 6.2–72.75 MΩ	Number of arc models	0
			R1(GΩ)	4.421
			R2(GΩ)	0.3
			C1(pF)	20
			C2(pF)	0.2
I_{max} = 0.8mA, THD = 11.70%, 5th dominant	I_{max} = 0.8 mA, THD = 11.70%, 5th dominant	$R_{nonlinear}$ range = 5.87–18.2 MΩ	Number of arc models	0

The simulation results demonstrate close alignment between the LC waveforms, magnitudes, and harmonic components of the simulations and those observed in the experiments. Therefore, the electrical circuit parameters employed to generate the LC profiles in the simulation are deemed valid and suitable for analysis. The LC profiles highlight that a higher pollutant's conductivity increases the LC magnitude but reduces the THD. This observation is further supported by the larger distortion formed on the crest of the 1.3 mS-LC waveform compared to that of the 3.6 mS-LC waveform.

The obtained electrical circuit parameters depict that the nonlinear resistance of the insulator with 1.3 mS-pollutants is higher than that of the insulator with 3.6 mS-pollutants, aligning with the increased LC magnitude. It is due to larger pollutants' conductivity and the lower surface resistance of the insulator, allowing enhanced current flow on the surface. The intrinsic resistance value (R1) remains consistent due to the identical insulator material. The intrinsic capacitance value (C1) is also unchanged, attributed to the uniform test voltage of 30 kV. Notably, both conditions exhibit no arcs in the LC waveform, leading to the absence of arc models. This absence is further reflected in the identical surface resistance value (R2), dependent on arcs occurring in the LC waveform.

4-2- LC Simulation Results of the Uncoated Ceramic Insulator

Table 3 depicts simulation results for the LC profiles of uncoated ceramic insulators with pollutants' conductivity of 1.3 mS and 3.6 mS, along with their respective electrical equivalent circuit parameters. Despite variations in pollutants' conductivity, the symmetrical LC profiles of uncoated ceramic insulators result in only a marginal 0.26% difference in THD values between the two waveform samples. Similar to the RTV-SiR-coated ceramic insulator, the nonlinear resistance of the uncoated sample with 1.3 mS pollutants exceeds that of the 3.6 mS pollutants. C1 remains constant as both samples were tested at the same voltage of 30 kV, and R1 is identical due to the same material. However, the presence of an arc near the crest in the LC waveform of the non-coated ceramic insulator necessitates the use of an arc circuit for both conditions.

Table 3. Comparison of LC profiles between experimental and simulated results for uncoated ceramic insulators with varying pollutants' conductivity
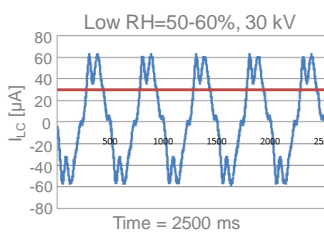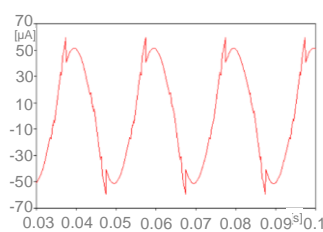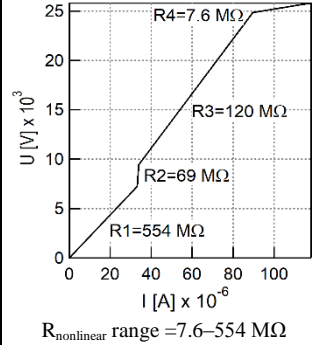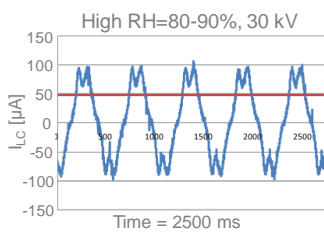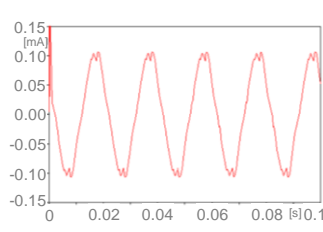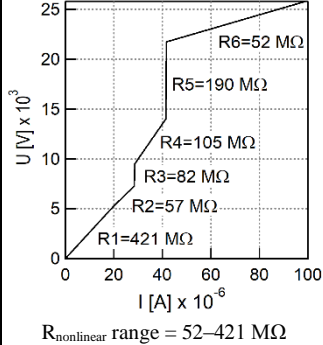
Leakage Current (LC) of Experiment	LC of Simulation	Electrical circuit parameters		
Pollutant 1.3 mS, 30 kV (waveform, Time = 2500 ms)	(waveform)	R5=5.59 MΩ, R4=4.67 MΩ, R3=9.59 MΩ, R2=6.28 MΩ, R1=10.89 MΩ	R1(GΩ)	4.421
			R2(GΩ)	0.3
			C1(pF)	15
			C2(pF)	0.05
I_{max} = 1.4 mA, THD = 11.44%, 5th dominant	I_{max} = 1.4 mA, THD = 11.23%, 5th dominant	$R_{nonlinear}$ range = 4.67–10.89 MΩ	Number of arc models	1
Pollutant 3.6 mS, 30 kV (waveform, Time = 2500 ms)	(waveform)	R5=3.25 MΩ, R5=4.74 MΩ, R4=3.64 MΩ, R3=3.28 MΩ, R2=5.16 MΩ, R1=10.89 MΩ	R1(GΩ)	4.421
			R2(GΩ)	0.3
			C1(pF)	15
			C2(pF)	0.05
I_{max} = 1.87 mA, THD = 11.70%, 5th dominant	I_{max} = 1.87 mA, THD = 11.78%, 5th dominant	$R_{nonlinear}$ range = 3.25–10.89 MΩ	Number of arc models	1

Compared to the RTV-SiR coated insulator, the nonlinear resistance parameter range of the uncoated ceramic insulator is lower. This is evident in the maximum values of $R_{nonlinear}$ at the same level of 3.6 mS-pollutants, i.e. 18.2 MΩ and 10.89 MΩ for the RTV-SiR coated and uncoated insulator, respectively. This difference allows for a larger LC magnitude flow on the uncoated insulator surface compared to the RTV-SiR coated one.

4-3- LC Simulation Results of the Epoxy Resin Insulator

Table 4 presents experimental and simulation results for epoxy resin insulator samples under varying relative humidity (RH) conditions, specifically low RH of 50-60% and high RH of 80-90%. In both conditions, the LC waveforms of the epoxy resin insulator samples exhibit symmetry, with distortions occurring at the peak. The distortion at the peak under low humidity conditions surpasses that under high humidity conditions, hence a higher THD value for the sample in low humidity. The LC magnitude demonstrates an increase with higher air humidity, as indicated by the maximum current (I_{max}) values of 0.06 mA for low humidity and 0.1 mA for high humidity.

Table 4. Comparison of LC profiles between experimental and simulated results for epoxy resin insulators with varying RH

Leakage Current (LC) of Experiment	LC of Simulation	Electrical circuit parameters		
			R1(GΩ)	36.38
			R2(GΩ)	0.3
			C1(pF)	5
			C2(pF)	1
I_{max} = 0.06 mA, THD = 18.5%, 5th dominant	I_{max} = 0.06 mA, THD = 18.4%, 5th dominant	$R_{nonlinear}$ range =7.6–554 MΩ	Number of arc models	1
			R1(GΩ)	36.38
			R2(GΩ)	0.3
			C1(pF)	5
			C2(pF)	5
I_{max} = 0.1 mA, THD = 15.85%, 5th dominant	I_{max} = 0.1 mA, THD = 15.5%, 5th dominant	$R_{nonlinear}$ range = 52–421 MΩ	Number of arc models	0
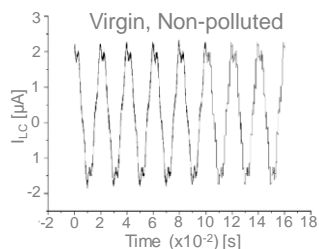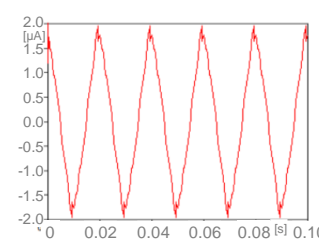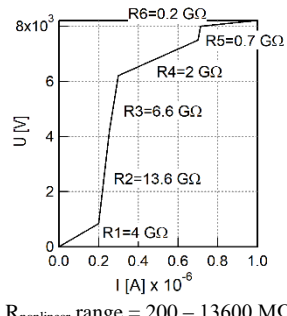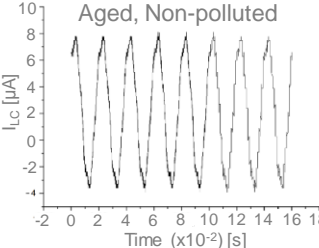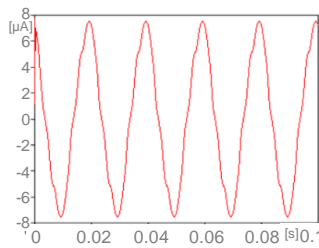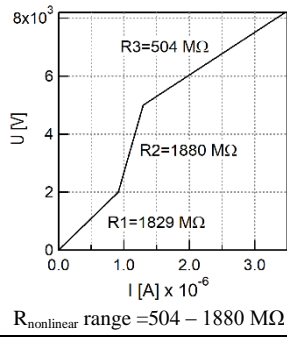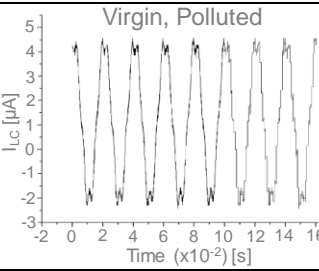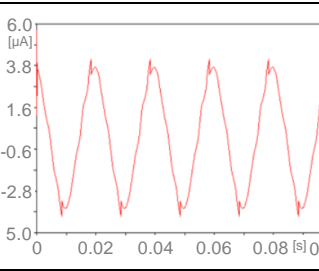
First of all, the intrinsic resistance (R1) of the epoxy resin polymer insulator is around 9 times larger (36 GΩ) than that of the ceramic insulators (4 GΩ). Thus, the range of LC magnitude of the polymer insulators also differs in the order of a few dozen µA, whereas that of the ceramic insulators is in the order of a few mA. Distinct characteristics of $R_{nonlinear}$ are observed under low and high humidity conditions, evident in the shapes of nonlinearity. The range is larger at 7.6-554 MΩ for lower humidity and smaller range at 52-421 MΩ for highe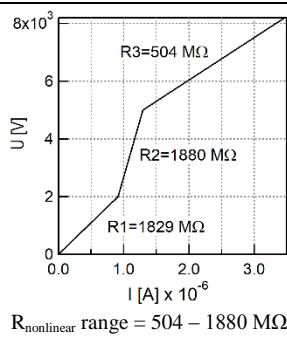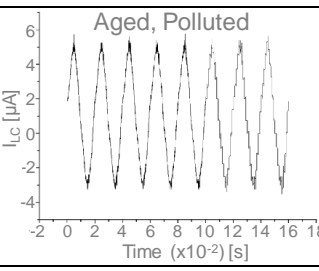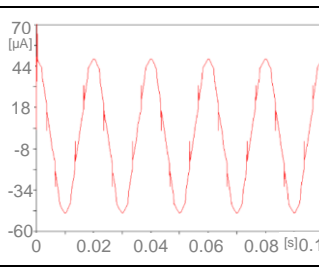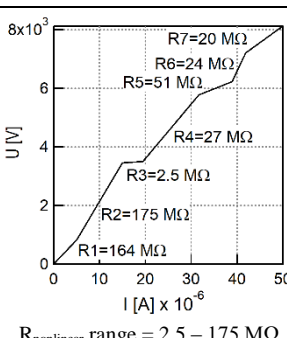r humidity. This difference is due to the elevated humidity surrounding the insulator, increasing the water content in the air and consequently enhancing the conductivity of the insulator surface while decreasing surface resistance [25]. Additionally, compared to silicone rubber, epoxy resin materials are more hydrophilic, making air with high humidity significantly influence the insulator's performance [26].

Regarding other parameters, the surface linear resistance (R2) maintains a constant value of 0.3 Ω for both high and low-humidity samples. The surface capacitance (C2) decreases from 5 pF to 1 pF under low humidity. The intrinsic capacitance value (C1) also remains constant at 5 pF for samples in both conditions, as they are tested at the same applied voltage.

4-4- LC Simulation Results of the Silicone Rubber Polymer Insulator

LC experiments were conducted on silicone rubber polymer insulators, exploring variations in age and pollutants. Table 5 displays the LC profiles from experiments and simulation results, revealing differences in insulator conditions due to age variation. The LC magnitude for the virgin insulator under non-polluted conditions is 2 µA, whereas, for the aged insulator under the same conditions, it increases to 7.13 µA—roughly three times larger than that of the virgin insulator. The waveform analysis indicates a distortion at the crest for the virgin insulator, while the aged insulator exhibits slight distortion around the crest neck. Both cases exhibit symmetrical waveform properties. Increased factors that may damage the insulator, such as aging and pollutants, lead to greater LC flow. Polymer insulators are more susceptible to aging effects compared to ceramic insulators due to potential changes in chemical composition under long-term electrical, mechanical, and environmental stresses. Consequently, polymer insulators experience decreased surface resistance, hydrophobicity, and erosion on the insulator surface [27].

Table 5. Comparison of LC profiles between experimental and simulated results for silicone rubber polymer insulators with varying age and pollutants

Leakage Current (LC) of Experiment	LC of Simulation	Electrical circuit parameters		
Virgin, Non-polluted (graph)	(graph)	(U-I graph: R6=0.2 GΩ, R5=0.7 GΩ, R4=2 GΩ, R3=6.6 GΩ, R2=13.6 GΩ, R1=4 GΩ)	R1(GΩ)	44.21
			R2(GΩ)	0.3
			C1(pF)	5 E-3
			C2(pF)	5E-3
I_{max} = 2 µA, THD = 13.3%, 5th dominant	I_{max} = 2 µA, THD = 13.2%, 5th dominant	$R_{nonlinear}$ range = 200 – 13600 MΩ	Number of arc models	1
Aged, Non-polluted (graph)	(graph)	(U-I graph: R3=504 MΩ, R2=1880 MΩ, R1=1829 MΩ)	R1(GΩ)	44.21
			R2(GΩ)	0.3
			C1(pF)	8E-3
			C2(pF)	9E-2
I_{max} = 7.2 µA, THD = 9.6%, 5th dominant	I_{max} = 7.13 µA, THD = 9.51%, 5th dominant	$R_{nonlinear}$ range =504 – 1880 MΩ	Number of arc models	0
Virgin, Polluted (graph)	(graph)	(U-I graph: R3=504 MΩ, R2=1880 MΩ, R1=1829 MΩ)	R1(GΩ)	44.21
			R2(GΩ)	0.3
			C1(pF)	8E-2
			C2(pF)	1E-3
I_{max} = 4.2 µA, THD = 12.87%, 5th dominant	I_{max} = 4.2 µA, THD = 12.86%, 5th dominant	$R_{nonlinear}$ range = 504 – 1880 MΩ	Number of arc models	1
Aged, Polluted (graph)	(graph)	(U-I graph: R7=20 MΩ, R6=24 MΩ, R5=51 MΩ, R4=27 MΩ, R3=2.5 MΩ, R2=175 MΩ, R1=164 MΩ)	R1(GΩ)	44.21
			R2(GΩ)	0.3
			C1(pF)	5E-2
			C2(pF)	5E-2
I_{max} = 0.05 mA, THD = 8.87%, 3rd Dominant	I_{max} = 0.049 mA, THD = 8.5%, 3rd Dominant	$R_{nonlinear}$ range = 2.5 – 175 MΩ	Number of arc models	0
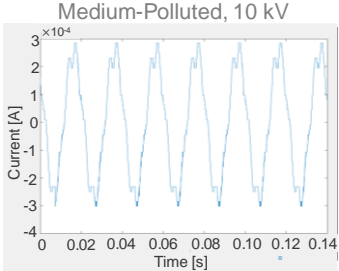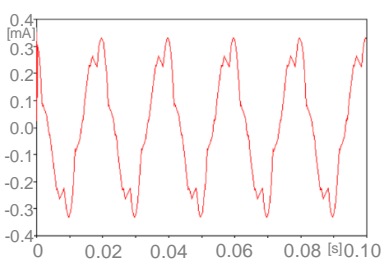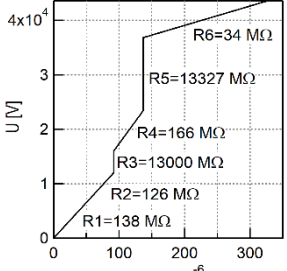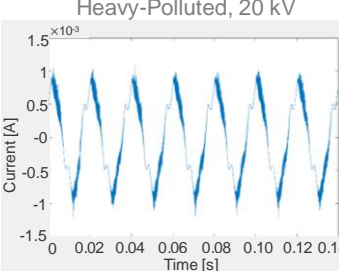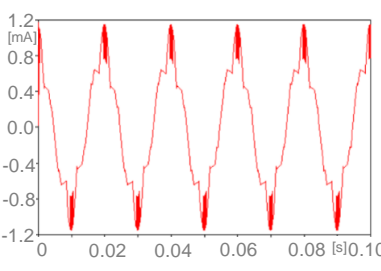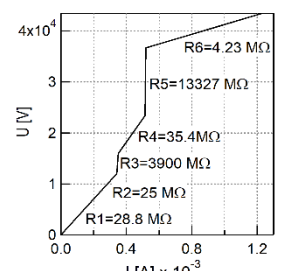
The LC properties are reflected in the electrical circuit parameter values presented in Table 5. Similar to the epoxy resin polymer insulator, the silicone rubber polymer insulator also has R1 in the range of a few dozen GΩ, i.e. 44.21 GΩ which is ten times larger than that of the ceramic insulator (4.42 GΩ). Thus, the range of LC magnitude is in the order of a few µA, even smaller than that of the epoxy resin insulator. The aged insulator exhibits a smaller range of $R_{nonlinear}$ (a few hundred to a few thousand MΩ) than the virgin insulator (a few hundred MΩ to dozens GΩ), attributed to the diminished surface material properties resulting from UV light exposure and environmental conditions during accelerated aging [15]. This decrease enhances surface conductivity, lowering the resistance and facilitating larger LC flow. The $R_{nonlinear}$ value of the aged and polluted insulator is the smallest among the conditions, ranging from 2.5-175 MΩ. This is a consequence of multiple factors damaging the insulator surface, including pollutants and aging [27]. Pollutants increase the likelihood of water coverage on the insulator surface, enhancing its conductivity. Consequently, the electrical circuit perceives a lower $R_{nonlinear}$ value. When considering all effects in Table 5, the influences of age as well as UV radiation are deemed more significant than that of pollutants.

As for other parameters, the linear resistance value of the insulator surface (R2) remains constant at 0.3 Ω. The virgin insulators have smaller insulator surface capacitance (C2) than the aged insulators. The choice of C2 value in virgin non-polluted conditions is based on the arc position, requiring the inclusion of an arc circuit due to significant distortion at the wave crest.

4-5- LC Simulation Results of the Glass Insulator

Table 6 shows the comparison between experimental and simulated LC profiles of glass insulators, along with the corresponding electrical circuit parameters defining the approximated insulator conditions. The table reveals congruent simulated waveforms, displaying identical LC magnitudes and THD values to the experimental data for each pollution condition. This validation attests to the accuracy of the obtained electrical circuit parameter values.

Table 6. Comparison of LC profiles between experimental and simulated results for glass insulators with varying pollutant levels
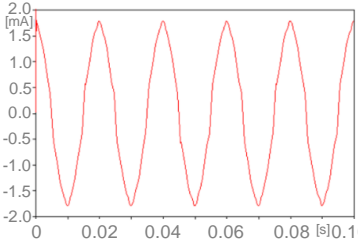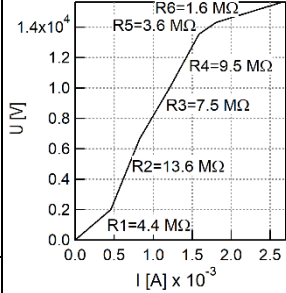
Leakage Current (LC) of Experiment	LC of Simulation	Electrical circuit parameters		
Medium-Polluted, 10 kV			R1(GΩ)	4.421
			R2(GΩ)	0.3
			C1(pF)	3
			C2(pF)	0.1
$I_{max} = 0.3$ mA, THD = 16.59%	$I_{max} = 0.3$ mA, THD = 16.55%	$R_{nonlinear}$ range = 34 – 13327 MΩ	Number of arc models	0
Heavy-Polluted, 20 kV			R1(GΩ)	4.421
			R2(GΩ)	0.3
			C1(pF)	5
			C2(pF)	0.1
$I_{max} = 1$ mA, THD = 17.28%	$I_{max} = 1.1$ mA, THD = 16.83%	$R_{nonlinear}$ range = 4.23 – 13327 MΩ	Number of arc models	1

In this simulation, a single circuit is employed to generate a symmetrical leakage current waveform. Glass insulator samples with lower LC magnitudes exhibit larger $R_{nonlinear}$ values, ranging from 4.23 to 13,327 MΩ. Regarding other circuit properties, the C1 value is influenced by the applied voltage, with a higher voltage corresponding to a higher C1 value. The values of C2 and R2 are contingent on the location of the occurred arcs on the waveform. The number of arc circuits used depends on the shape of arcs present in the LC waveform.

4-6- LC simulation Results of the Semiconducting Glazed Insulator

The final set of results pertains to the LC simulation of the SCG insulator under varying pollutant levels, including the electrical circuit parameters outlined in Table 7. Among the electrical circuit properties of the SCG insulator, the $R_{nonlinear}$ of the non-polluted sample exhibits a remarkably higher value compared to the sample with medium pollutants, aligning with the LC magnitude obtained from the experiments. It is noteworthy that pollutants do not impact the surface resistivity (R2) of the SCG insulator. In comparison to glass insulators, the SCG insulator features a smaller and narrower range of $R_{nonlinear}$, spanning from 1.95M to 15.5MΩ

Table 7. Comparison of LC profiles between experimental and simulated results for SCG insulators with varying pollutant levels

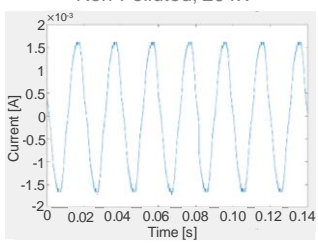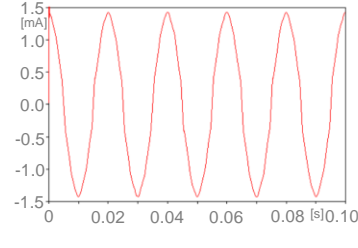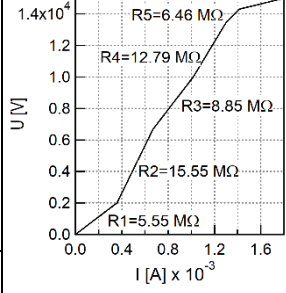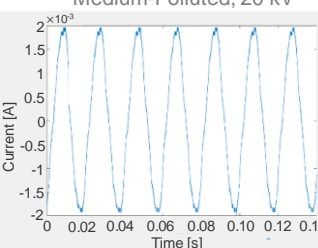| Leakage Current (LC) of Experiment	LC of Simulation	Electrical circuit parameters		
Non-Polluted, 20 kV (graph)	(graph)	R6=1.95 MΩ, R5=6.46 MΩ, R4=12.79 MΩ, R3=8.85 MΩ, R2=15.55 MΩ, R1=5.55 MΩ	R1(GΩ)	1.04
			R2(GΩ)	0.3
			C1(pF)	1
			C2(pF)	0.1
I_{max} = 1.5mA, THD = 6.37%	I_{max} = 1.5mA, THD = 6%	$R_{nonlinear}$ range = 1.9 – 15.55 MΩ	Number of arc models	0
Medium-Polluted, 20 kV (graph)	(graph)	R6=1.6 MΩ, R5=3.6 MΩ, R4=9.5 MΩ, R3=7.5 MΩ, R2=13.6 MΩ, R1=4.4 MΩ	R1(GΩ)	1.04
			R2(GΩ)	0.3
			C1(pF)	1
			C2(pF)	0.1
I_{max} = 1.5mA, THD = 6.37%	I_{max} = 1.5mA, THD = 6%	$R_{nonlinear}$ range = 1.6 – 13.6 MΩ	Number of arc models	0

5- Analysis and Discussions

The comparison of insulator intrinsic, insulator surface, and arc circuit parameters for different types of insulators is tabulated in Table 8, showcasing the range of values for each parameter along with the maximum number of required arc models.

The nonlinear surface resistance ($R_{nonlinear}$) values for ceramic insulators generally fall within the mega-ohm range, whereas those for epoxy resin insulators range from tens to hundreds of mega-ohms, and polymer insulators exhibit values in the range of tens of mega-ohms to 13 giga-ohms. This suggests that, for minimizing LC on insulator surfaces due to the pollutant effect, silicone rubber polymer insulators, with their higher surface resistance compared to ceramic and epoxy resin polymer insulators, can be effectively utilized.

The intrinsic resistance value R1 is standardized for insulating materials of the same type, serving as a distinguishing factor between insulating materials. Polymer insulators, made of either silicone rubber or epoxy resin material, have the largest intrinsic resistance when compared to conventional ceramic or glass insulators [16]. The resistance value of epoxy resin insulators is obtained from the ratio between the LC magnitude of epoxy resin and that of ceramic insulators [26]. The value of R2 remains constant for all insulator types regardless of the various conditions, as the arc position is regulated by other circuit parameters, i.e., C2, R(i), and the number of arc models.

Table 8. Comparison of intrinsic parameters between insulator types

Insulator Types	R(i) (MΩ)	R1 (GΩ)	R2(Ω)	C1(pF)	C2(pF)	N Arc
RTV-SiR-Coated Ceramic	5.87-72.75	4.421	0.3	20	0.1-0.2	0
Non-coated Ceramic	3.25-10.89	4.421	0.3	15	0.005	1
Epoxy Resin	7.6-554	36.38	0.3	5	1-5	0-1
Silicon Rubber Polymer	2.5-13600	44.21	0.3	0.005-0.08	0.001-0.09	0-1
Glass	4.23-13327	4.421	0.3	3-5	0.1	1
Semi-conducting Glaze	1.95-15.5	1.04	0.3	1	0.1	0

The surface capacitance C2 values vary among different types of insulators, with silicone rubber polymer insulators exhibiting the smallest value and epoxy resin insulators having the largest value. C2's value is influenced by the arc position, as a larger surface capacitance causes a delay in the occurrence of arcs on the waveform. Consequently, C2 serves as an adjustment factor for the arc position on the waveform.

Regarding the number of arc models, the RTV-SiR-coated insulator has the minimum number. Compared to the uncoated insulator, it requires fewer arc models due to less extreme test conditions, i.e., less arc activities, and the RTV-SiR coating's characteristic reduces dry-band arcing, eliminating the need for an arc circuit. Therefore, the appearance of arcs is minimal through the protective coating. Overall, the limited number of arc models results from the scarcity of arcs in the LC waveforms, also maintaining the surface resistance parameters unchanged.

6- Conclusions

Leakage current (LC) tests were conducted on various outdoor insulators, including room-temperature vulcanized-silicone rubber (RTV-SiR)-coated and uncoated ceramic insulators, epoxy resin polymer insulators, silicone rubber polymer insulators, glass insulators, and semiconducting glaze (SCG) insulators. Experiments incorporated different environmental conditions, including varying pollutant levels affecting insulator conductivity, humidity variations, and UV radiation for the aging effect. Computer simulations utilizing LC equivalent circuits successfully reproduced similar LC waveforms at each condition, evident in matched LC magnitude, THD, and dominant harmonic numbers. The key findings are as follows:

- Intrinsic resistance values differ among insulating materials, with SiR polymer material having the largest resistance among all types.

- Nonlinear resistance, a vital parameter reflecting environmental effects, decreases with heightened insulator stress, leading to increased surface current. SiR polymer insulators also exhibit the highest nonlinear resistance, followed by glass, epoxy resin, RTV-SiR-coated ceramic, uncoated ceramic, and SCG insulators.

- Surface capacitance parameters show variability, determined by the arc location in the simulated LC waveform.

- Fixed linear surface resistance values were consistent across all conditions and insulator types, facilitating a comprehensive parameter analysis.

Monitoring nonlinear resistance provides a viable method for insulator condition assessment. Silicone rubber polymer insulators demonstrate superior characteristics in minimizing leakage current due to pollutant accumulation. Other circuit parameters are influenced by both the nature of the insulator material and specific insulator conditions.

Deriving LC equivalent circuit parameters from diverse LC waveforms provides a comprehensive understanding of the electrical characteristics of various insulator types and the impact of pollutants on insulator surface conditions. Particularly, the nonlinearity resistance and the number of arc models elucidate the occurrence of arc phenomena on the insulator surface. The primary challenge lies in collecting data from LC measurements under varying combinations of environmental factors for different insulator types. However, upon completion, simulation results specifying LC magnitude levels, waveform symmetry, harmonic components, and THD levels can be utilized to assess severity levels, ranging from normal to pre-flashover. Future development aims to leverage the database for controlling arc activities on insulator surfaces through coating material modifications, such as nanocoating applications.

7- Declarations

7-1- Author Contributions

Conceptualization, A.B. and S.; methodology, A.B.; software, A.B.; validation, A.B.; formal analysis, A.B. and R.; investigation, A.B.; resources, S.; data curation, A.B. and R.; writing—original draft preparation, A.B.; writing—review and editing, R.; visualization, R.; supervision, S.; project administration, S.; funding acquisition, S. All authors have read and agreed to the published version of the manuscript.

7-2- Data Availability Statement

The data presented in this study are available in the article.

7-3- Funding

The authors received financial support from Institut Teknologi Bandung, Indonesia for the research and publication of this article.

7-4- Institutional Review Board Statement

Not applicable.

7-5- Informed Consent Statement

Not applicable.

7-6- Conflicts of Interest

The authors declare that there is no conflict of interest regarding the publication of this manuscript. In addition, the ethical issues, including plagiarism, informed consent, misconduct, data fabrication and/or falsification, double publication and/or submission, and redundancies have been completely observed by the authors.

8- References

[1] Sharma, K. (2001). Polymeric insulators. Technical Article, 1-28. Available online: http://www.appstate.edu/~clementsjs/ surfaceflashover/insulatortesting.pdf (accessed on June 2023).

[2] Serikbay, A., Bagheri, M., & Zollanvari, A. (2023). Stacked Ensemble Deep Learning for Outdoor Insulator Surface Condition Classification: A Profound Study on Water Droplets. IEEE Access, 11, 102279–102289. doi:10.1109/ACCESS.2023.3315599.

[3] Busby, J. W., Baker, K., Bazilian, M. D., Gilbert, A. Q., Grubert, E., Rai, V., Rhodes, J. D., Shidore, S., Smith, C. A., & Webber, M. E. (2021). Cascading risks: Understanding the 2021 winter blackout in Texas. Energy Research and Social Science, 77, 102106. doi:10.1016/j.erss.2021.102106.

[4] Hussain, M. M., Farokhi, S., McMeekin, S. G., & Farzaneh, M. (2015). Dry band formation on HV insulators polluted with different salt mixtures. 2015 IEEE Conference on Electrical Insulation and Dielectric Phenomena (CEIDP), Michigan, United States. doi:10.1109/ceidp.2015.7352000.

[5] Kumara, S., & Fernando, M. (2020). Performance of outdoor insulators in tropical conditions of Sri Lanka. IEEE Electrical Insulation Magazine, 36(4), 26–35. doi:10.1109/MEI.2020.9111097.

[6] Butt, S. U., Khattak, A., Ali, A., Faiza, Imran, K., Ullah, N., Alahmadi, A. A., & Khan, A. (2021). Investigation of epoxy composites for outdoor insulation under accelerated ultraviolet exposure. Materials Research Express, 8, 1-15. doi:10.1088/2053-1591/ac1aa8.

[7] Liu, L., Guo, C., Xiang, Y., Tu, Y., Mei, H., Wang, L., & Xuan, F. Z. (2022). Health Monitoring of RTV Silicone Rubber Coating on Insulators Based on Multimode Features of Active Infrared Thermography. IEEE Transactions on Instrumentation and Measurement, 71, 4502609. doi:10.1109/TIM.2022.3164159.

[8] Xin, L., Jin, H., Tu, Y., Yuan, Z., Lv, Z., & Wang, C. (2020). Defect Detection and Characterization of RTV Silicone Rubber Coating on Insulator Based on Visible Spectrum Image. IEEE Transactions on Power Delivery, 35(6), 2734–2736. doi:10.1109/TPWRD.2020.2995071.

[9] Waluyo, Fauziah, D., & Khaidir, I. M. (2021). The Evaluation of Daily Comparative Leakage Currents on Porcelain and Silicone Rubber Insulators under Natural Environmental Conditions. IEEE Access, 9, 27451–27466. doi:10.1109/ACCESS.2021.3057626.

[10] Salem, A. A., Lau, K. Y., Rahiman, W., Abdul-Malek, Z., Al-Gailani, S. A., Rahman, R. A., & Al-Ameri, S. (2022). Leakage current characteristics in estimating insulator reliability: experimental investigation and analysis. Scientific Reports, 12(1), 14974. doi:10.1038/s41598-022-17792-x.

[11] Obenaus, F. (1958). Contamination flashover and creepage path length. Deutsch - Elektrotechnik, 12, 135-136.

[12] Vosloo, W. L., & Holtzhausen, J. P. (2002). A model for electrical discharge and leakage current development on high voltage insulators. Proceedings of the Second IASTED International Conference Power and Energy Systems, 25-28 June 2002, Crete, Greece.

[13] Pratomosiwi, F., & Suwarno. (2009). Electrical equivalent circuit of ceramics insulators with RTV Silicone Rubber coated and computer simulation of leakage current. 2009 International Conference on Electrical Engineering and Informatics. doi:10.1109/iceei.2009.5254748.

[14] Rachmawati, R., Sartika, N., Meisa Putra, N. R., & Suwarno, S. (2018). The Study on Leakage Current Characteristics and Electrical Properties of Uncoated Ceramic, RTV Silicon Rubber Coated Ceramic, and Semiconducting Glazed Outdoor Insulators. International Journal on Electrical Engineering and Informatics, 10(2), 318–336. doi:10.15676/ijeei.2018.10.2.9.

[15] Wakhidin, M., & Suwarno. (2019). Effects of Artificial Tropical Climate Aging on Insulation Performance of Silicone Rubber Polymeric Insulators. 2019 2nd International Conference on High Voltage Engineering and Power Systems (ICHVEPS), Bali, Indonesia. doi:10.1109/ichveps47643.2019.9011130.

[16] Lumba, L. S., & Suwarno, S. (2020). Analysis of Surface Degradation of Silicon Rubber Insulators after 30 Years in-Service. International Journal on Electrical Engineering and Informatics, 12(4), 828–844. doi:10.15676/ijeei.2020.12.4.8.

[17] IEC-507. (1991). Artificial Pollution Tests on High-Voltage Insulators to be used on A.C. Systems. International Electrotechnical Commission (IEC), Geneva, Switzerland.

[18] ANSI C.29 13. (2000). American National Standard for Insulators-Composite-Distribution Dead-end Type. American National Standards Institute (ANSI), Washington, United States.

[19] IEC 60507. (2013). Artificial pollution tests on high-voltage ceramic and glass insulators to be used on A.C. systems. International Electrotechnical Commission (IEC), Geneva, Switzerland.

[20] Kizilcay, M., & Pniok, T. (1991). Digital simulation of fault arcs in power systems. European Transactions on Electrical Power, 1(1), 55–60. doi:10.1002/etep.4450010111.

[21] Kumar, K., Maheswari, R. V., & Vigneshwaran, B. (2020). Investigation of Pollution Severity and Dry Band Characteristics on 11kV Composite Insulator. In 2020 IEEE International Conference on Advances and Developments in Electrical and Electronics Engineering (ICADEE), 1-6. doi:10.1109/ICADEE51157.2020.9368945.

[22] He, J., He, K., & Gao, B. (2019). Modeling of dry band formation and arcing processes on the polluted composite insulator surface. Energies, 12(20), 3905. doi:10.3390/en12203905.

[23] Nigol, O., & Cherney, E. A. (1975). Development and application of a new semiconductive glaze insulator. EIC 12th Electrical / Electronics Insulation Conference. doi:10.1109/eic.1975.7458534.

[24] Cherney, E. A., Nigol, O., & Reichman, J. (1978). Development and application of a new semiconductive-glaze insulator. IEEE Transactions on Power Apparatus and Systems, PAS-97(6), 2117–2126. doi:10.1109/TPAS.1978.354715.

[25] Deb, S., Ghosh, R., Dutta, S., Dalai, S., & Chatterjee, B. (2017). Effect of humidity on leakage current of a contaminated 11 kV Porcelain Pin Insulator. 6th International Conference on Computer Applications in Electrical Engineering-Recent Advances (CERA), Roorkee, India. doi:10.1109/cera.2017.8343329.

[26] Syakur, A., Berahim, H., & Rochmadi, T. (2012). Leakage current monitoring for silane epoxy resin insulator under tropical climate conditions. 2012 IEEE International Conference on Condition Monitoring and Diagnosis, Bali, Indonesia. doi:10.1109/cmd.2012.6416291.

[27] Ashwini, A. V., Ravi, K. N., & Vasudev, N. (2019). Experimental Study on Aging of Polymeric Insulators by Dip Method. International Conference on High Voltage Engineering and Technology, Hyderabad, India. doi:10.1109/ichvet.2019.8724262.